

Journal of  
**APPLIED PHYSICS**

Proceedings of the Thirty-First  
Annual Conference on Magnetism  
and Magnetic Materials  
Pages 3781-4446

Volume 61

15 April 1987

Number 8, Part IIB

a publication of the American Institute of Physics

**PROCEEDINGS OF THE THIRTY-FIRST  
ANNUAL CONFERENCE ON MAGNETISM  
AND MAGNETIC MATERIALS**

**PART B**

**17–20 November 1986  
Baltimore, Maryland**

**Edited by N. C. Koon, J. D. Adam,  
I. A. Beardsley, and D. L. Huber**

**Journal of Applied Physics  
Volume 61, Number 8, Part II, 1987**

# Effect of defects and further neighbor interactions on a two-dimensional dipolar system on a honeycomb lattice

George O. Zimmerman and A. K. Ibrahim  
 Physics Department, Boston University, Boston, Massachusetts 02215

F. Y. Wu  
 Physics Department, Northeastern University, Boston, Massachusetts 02115

A theoretical investigation of a planar dipolar system on a honeycomb lattice reveals that the ground-state energy is increased for finite systems over that of an infinite system. The infinite system has a ground-state degeneracy with respect to dipole orientations. This degeneracy is lifted for finite systems. A mean-field calculation including nearest, second, and third neighbors shows that there are three phases, an ordered phase, a paramagnetic one, and a magnetic-field-induced ferromagnetic phase. A defect in the second nearest neighbor has the effect of introducing a finite magnetization at zero field at low temperatures.

## INTRODUCTION

One can show that in a perfect dipolar honeycomb lattice of infinite extent and at zero temperature, the ground state is infinitely degenerate.<sup>1</sup> Figure 1 shows one of a degenerate configurations from which all the others can be derived. One can decompose the lattice into elementary hexagons, with the six dipoles numbered 1, 1', 2, 2', 3, and 3' constituting one of those. In the figure those with  $N$  denote the next, second, and third nearest neighbor to the initial hexagon. Dipoles with the same number have the same orientation. From this configuration one obtains all the other states with identical energies by rotating the unprimed dipoles by the same arbitrary angle clockwise while the primed dipoles are rotated by the same angle in the counterclockwise direction or vice versa. It is thus of interest to explore if defects or boundaries favor one of the ground states over another.<sup>2</sup> In the same paper,<sup>1</sup> a mean-field calculation was performed which extended the behavior of the system to finite

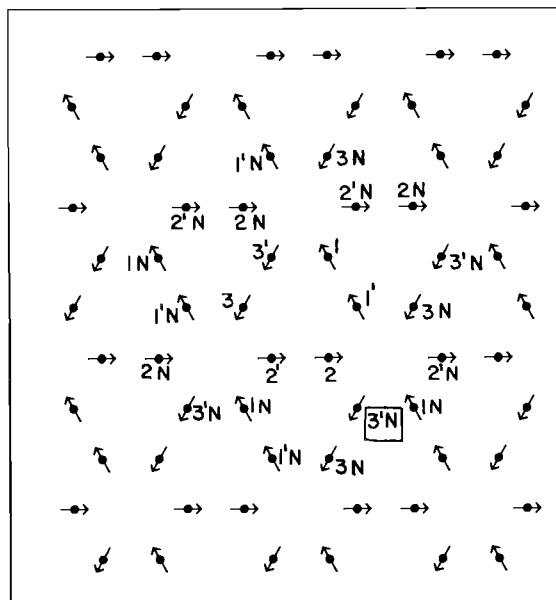


FIG. 1. Lattice with ground-state dipole directions.  $N$  denotes neighbors of the main hexagon taken into account in the mean-field calculation.

temperatures and finite magnetic fields. That calculation, which was confined to the first nearest neighbors only, showed that the system has a critical point at zero field where it undergoes a transition from an ordered to a disordered state and that transition can be traced as a function of an applied magnetic field. The change of phase is marked by susceptibility and specific heat maxima.

## METHOD OF CALCULATION

The ground-state energy calculations of an infinite and the finite systems was performed by summing the interactions of each dipole with all the others in the lattice. In these calculations we used the usual expression for the dipolar energy

$$U_{ij} = \frac{\boldsymbol{\mu}_i \cdot \boldsymbol{\mu}_j}{r_{ij}^3} - \frac{3(\boldsymbol{\mu}_i \cdot \mathbf{r}_{ij})(\boldsymbol{\mu}_j \cdot \mathbf{r}_{ij})}{r_{ij}^5}. \quad (1)$$

If the dipoles are identical, one can rewrite (1) in terms of unit vectors as shown in Eq. (2):

$$U_{ij} = J_{ij} [ \hat{\boldsymbol{\mu}}_i \cdot \hat{\boldsymbol{\mu}}_j - 3(\hat{\boldsymbol{\mu}}_i \cdot \hat{\mathbf{r}}_{ij})(\hat{\boldsymbol{\mu}}_j \cdot \hat{\mathbf{r}}_{ij}) ]. \quad (2)$$

From now on we use dimensionless units where  $J = 1$  for nearest neighbors, the temperature is given in units of  $J$ , the distance between two nearest neighbors (ND) will be taken as one, and the magnetic field  $h$  will be in units of  $(\mu H / J)$ .

The mean-field calculation was performed by self-consistently solving the equations of Lee *et al.*<sup>3</sup> modified for dipolar interactions. In that method the free energy, given in Eq. (3), is minimized:

$$F(\rho) = k_B T \text{Tr} \left[ \rho \left( K \sum_{ij} U_{ij} - h \cdot \sum_i \boldsymbol{\mu}_i + \ln \rho \right) \right]. \quad (3)$$

In this equation  $F$  denotes the free energy,  $\rho$  is the density matrix,  $K = J/k_B T$ , and  $h = H\mu/k_B T$ . This minimization gives an expression for the magnetization of a dipole given by Eq. (4):

$$\mathbf{m}_i = m(a_i) \hat{\mathbf{a}}_i, \quad (4)$$

where  $m(a) = I_1(a)/I_0(a)$ , and  $I_n(a)$  is the modified Bessel function of order  $n$ . The vectors  $\mathbf{a}_i$  are mean-field parameters that are determined from the self-consistent equations

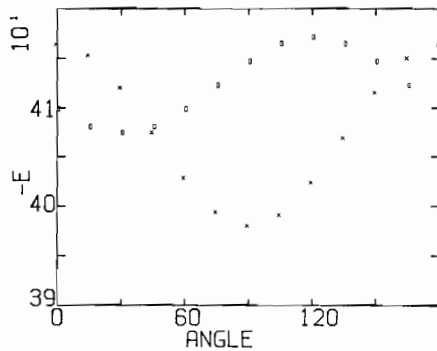


FIG. 2. Energy per dipole pair of the square ( $\times$ ) and the circular ( $\square$ ) array of dipoles, as a function of the angle of dipole No. 2.

$$\mathbf{a}_i = \mathbf{h} - K \sum_j' m(a_j) [\hat{a}_j - 3\hat{r}_{ij}(\hat{a}_j \cdot \hat{r}_{ij})], \quad (5)$$

where the prime over the summation sign denotes the restriction that  $i \neq j$ . An iterative solution of Eq. (5) provides self-consistent values of  $a_i$  from which  $F$ , the free energy,  $M$ , the magnetization, and  $S$ , the entropy, can be obtained for any temperature and applied magnetic field. The magnetic susceptibility and the specific heat can then be obtained by simple numerical differentiation.

### THE GROUND STATE

The calculation of the energy per dipole was carried out as described in the previous section. For an infinite lattice the energy per dipole is  $E = -2.25$ .

A finite array raises the energy of the system. Moreover, that energy is, to a small degree, dependent on the orientation of the dipoles. As an example, we calculated the energies of two such arrays. The first was 170 dipoles arranged on a square with a side length of 15.5 ND; the other was an array of 180 dipoles contained within a circle of 17 ND. In both of these arrays 20% of the dipoles were on the boundary, where the boundary dipoles were defined as those that were missing at least one nearest neighbor. The average energy per dipole pair,  $E$ , is shown in Fig. 2 for both arrays as a function of spin orientation. The angle, in degrees, denotes the "2" dipole orientation. For the square the average minimum energy per dipole pair was  $-4.169$ , while the maximum was  $-4.072$ ;

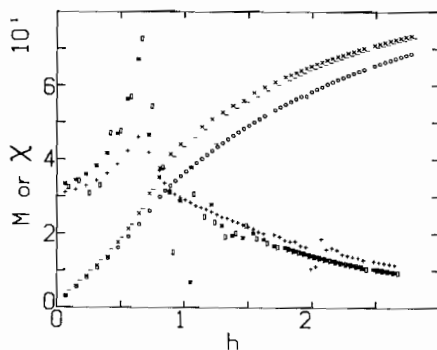


FIG. 3. Magnetization and susceptibility at  $T = 2$  as a function of the applied field. For the magnetization the circle,  $\times$ , and  $-$  denote the nn, nnn, and the nnd calculations, respectively, while the susceptibilities are given by  $+$ , box, and star.

for the circle the values were  $-4.151$  and  $-3.978$ , respectively.

### MEAN-FIELD CALCULATION

In Ref. 1 we calculated the behavior of the system taking into account only the nearest-neighbor interactions. Thus the interactions of the central hexagon containing the dipoles numbered 1, 1', 2, 2', 3, and 3' in Fig. 1, and the nearest neighbors of each of them were taken into account. In this approximation, a primed dipole, as shown in Fig. 1, interacted only with an unprimed one and vice versa. Since in a honeycomb lattice, with nearest-neighbor distance 1 ND, the second nearest neighbors are  $\sqrt{3}$  ND away, while the third neighbors are 2 ND away, they contribute significantly to the interaction. The calculation was thus extended to also include second and third nearest neighbors. The magnetization and susceptibility calculated in this manner are shown in Fig. 3 for a temperature of  $T = 2$  and as a function of the applied magnetic field. This figure shows our present calculation, as well as our previous results that contained only the nearest neighbors, for comparison.

One notes that the nearest-neighbor calculations (nn) give a lower magnetization than those including second and third nearest ones (nnn). The sharp and large maximum in the susceptibility, here seen at  $h = 0.7$  and then a less pronounced peak near  $h = 1.6$ , indicate transitions from phase I to phase II and from phase II to phase III, respectively.

If one maps those phases on the temperature-magnetic-field plane, one obtains Fig. 4. Here the boxes denote the phase I-II transition, while the stars denote the phase II-III transition, as calculated for nearest neighbors only. The  $\times$  and the  $+$ , respectively, denote the same transitions for the nnn calculation. Phase I is the ordered phase, where dipolar interactions dominate. Phase II is the paramagnetic phase, while phase III is a field-induced ferromagnetic phase.

The nnn calculation was repeated with one of the second nearest neighbors to the central hexagon eliminated. The eliminated dipole is indicated in Fig. 1 by the small box. Thus, of the 18 neighbors of the central hexagon, one is missing. One thus introduces a defect in the lattice; we shall call this calculation nnd. The magnetization and susceptibility given by this calculation are shown in Fig. 3 and are denoted by  $-$  and a star. Both the overall magnetization and the

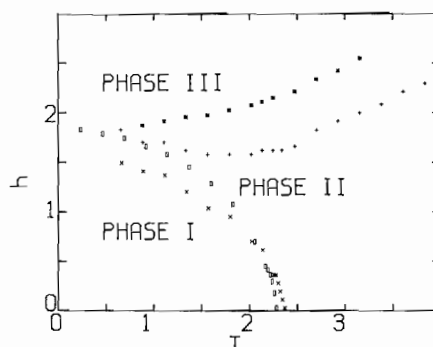


FIG. 4. Phase diagram of the system with the phases described in the text. The boxes and the  $*$  denote the nn calculation, while  $\times$  and  $+$  show the nnn and nnd results.

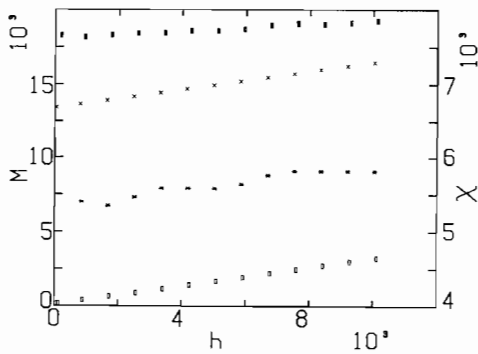


FIG. 5. Low-field behavior of the magnetization and susceptibility at  $T = 2$ . The open box and  $\times$  denote nnn and nnd magnetization, while the filled box and star denote the susceptibility.

susceptibility of this calculation are similar to the nnn results. However, the magnetization of the nnd is generally greater in phase I, the same in phase II, and smaller in phase III, as compared to that of nnn. The phase boundaries appear to be unaffected by the defect.

In nnd there is a finite magnetization at zero and low fields. Once the defect is introduced, it provides a focus for polarization. Thus at low fields the defects enhance the magnetization. As the field and temperature are raised, the influence of the defect becomes insignificant and thus the equality between the nnn and nnd results in phase II. In phase III the defect provides a disturbance in the lattice regularity and acts as a cavity in a ferromagnetic system, decreasing the overall magnetization, thus the lower magnetization in phase III. Figure 5 shows this effect in greater detail for the low-field region where both the magnetization and susceptibility are plotted for the nnn, open box and filled box, and nnd,  $\times$ , and star calculations. The figure shows that in nnn the magnetization goes to zero in zero field, while it is finite in the nnd case. In the nnd case the susceptibility, shown here with 0.3 subtracted from the actual value, has a small

minimum at low fields, while in nnn it is a monotonically increasing function in the low-field region.

## CONCLUSIONS

The inclusion of boundaries in a system of dipoles confined to rotate in a plane and located on a honeycomb lattice raises the average ground-state energy. Moreover, depending on the shape of the boundaries, the average ground-state energy depends on the dipole orientation.

The inclusion of second and third nearest neighbors in the interaction alters the phase boundaries of the system. Defects introduce a finite magnetization at low temperature, even at zero field. In low fields the susceptibility appears to have a minimum with respect to field at constant temperature for calculations including defects, while it is a monotonically increasing function of the field when no defects are included.

The system studied might be applicable to some two-dimensional systems where dipolar interactions play an important role. For one, such systems might be found in graphite intercalated compounds where a magnetic substance is the intercalant. The graphite layers thus reduce the interaction between the intercalant layers, creating a magnetic two-dimensional array within each intercalant layer.

## ACKNOWLEDGMENTS

G. O. Z. and A. K. I. were supported by the Air Force Office of Scientific Research under Grant No. AFOSR-82-0286. F. Y. W. was supported by the National Science Foundation under Grant No. DMR-8219254.

<sup>1</sup>G. O. Zimmerman, A. K. Ibrahim, and F. Y. Wu (unpublished).

<sup>2</sup>C. L. Henley (unpublished).

<sup>3</sup>D. H. Lee, R. G. Caflisch, J. D. Joannopoulos, and F. Y. Wu, Phys. Rev. B **29**, 2680 (1984).